

## Structure of Bayerite-Based Lithium–Aluminum Layered Double Hydroxides (LDHs): Observation of Monoclinic Symmetry

Sylvia Britto and P. Vishnu Kamath\*

Department of Chemistry, Central College, Bangalore University, Bangalore 560 001, India

Received August 21, 2009

The double hydroxides of Li with Al, obtained by the imbibition of Li salts into bayerite and gibbsite—Al(OH)<sub>3</sub>, are not different polytypes of the same symmetry but actually crystallize in two different symmetries. The bayerite-derived double hydroxides crystallize with monoclinic symmetry, while the gibbsite-derived hydroxides crystallize with hexagonal symmetry. Successive metal hydroxide layers in the bayerite-derived LDHs are translated by the vector ( $\sim -1/3, 0, 1$ ) with respect to each other. The exigency of hydrogen bonding drives the intercalated Cl<sup>−</sup> ion to a site with 2-fold coordination, whereas the intercalated water occupies a site with 6-fold coordination having a pseudotrigonal prismatic symmetry. The nonideal nature of the interlayer sites has implications for the observed selectivity of Li–Al LDHs toward anions of different symmetries.

### Introduction

The structure of aluminum hydroxide, Al(OH)<sub>3</sub>, comprises a close packing of hydroxyl ions in which two-thirds of the octahedral sites in alternative layers are occupied by Al<sup>3+</sup> ions, resulting in a stacking of charge neutral layers having the composition [Al<sub>2/3</sub>□<sub>1/3</sub>(OH)<sub>2</sub>] (□: cation vacancy). Incorporation of Li<sup>+</sup> into these ordered vacancies gives rise to positively charged layers having the composition [Al<sub>2/3</sub>Li<sub>1/3</sub>(OH)<sub>2</sub>]<sup>1/3+</sup>. Charge neutrality is restored by the incorporation of exchangeable anions in the interlayer region, yielding the I–III layered double hydroxides (LDHs) having the composition [Li<sub>0.33</sub>Al<sub>0.66</sub>(OH)<sub>2</sub>][A<sup>n−</sup>]<sub>0.33/n</sub>·xH<sub>2</sub>O (A = Cl<sup>−</sup>, NO<sub>3</sub><sup>−</sup>, SO<sub>4</sub><sup>2−</sup>, CO<sub>3</sub><sup>2−</sup>, and others).

The mechanism of formation of these LDHs has been shown to be through an “imbibition”<sup>2</sup> process in which the Li<sup>+</sup> ions diffuse into the Al(OH)<sub>3</sub> layers through the triangular faces of the [□(OH)<sub>6</sub>] octahedra by a mechanism known as diadochy.<sup>3</sup> The topotactic nature of this process implies that the structure of the LDH should be closely related to that of Al(OH)<sub>3</sub>. Al(OH)<sub>3</sub> crystallizes in four different polymorphic modifications, namely, gibbsite,<sup>4</sup> bayerite,<sup>5</sup> nordstrandite,<sup>6</sup> and doyleite,<sup>7</sup> of which the most common are gibbsite and bayerite. The main difference between these two polymorphs is in the stacking sequence

of the layers.<sup>8</sup> If the hydroxyl ion positions are represented by the upper-case symbols A and B, the stacking sequence in bayerite approximates to ABABAB..., giving one layer per unit cell. In gibbsite, adjacent layers are stacked one above the other in an eclipsed manner (ABBA ABBA...) to give two layers per unit cell.

Recently, it was shown by Besserguenev and co-workers<sup>9</sup> that the imbibition of Li salts into gibbsite results in a hexagonal LDH in which the layers are stacked one above the other in an eclipsed manner similar to that in gibbsite. The structure of the LDH obtained by soaking bayerite in Li salts is still uncertain. In an early paper, Poepelmeier and Hwu,<sup>2</sup> indexed the PXRD pattern of this phase to a hexagonal cell. Fogg and co-workers<sup>10</sup> indexed the PXRD pattern of this material to a rhombohedral cell with the layers stacked in an *abc abc...* manner (*a*, *b*, and *c* represent three separate metal hydroxide layers). This implies that, unlike the gibbsite-based LDHs, the bayerite-based LDHs do not conserve the stacking sequence of the parent phase. However, a closer look reveals that the indexing proposed by these authors<sup>10</sup> is incorrect, as we will show later in this paper. Since bayerite crystallizes with monoclinic symmetry, we considered the possibility that this symmetry is preserved in the LDH.

The Li–Al LDHs are unique among the wider class of layered hydroxides, for their important applications in catalysis<sup>11</sup> and in particular their tendency to exhibit

\*To whom correspondence should be addressed. E-mail: vishnukamath8@hotmail.com.

(1) Serna, C. J.; Rendon, J. L.; Iglesias, J. E. *Clays Clay Miner.* **1982**, *30*, 180.  
(2) Poepelmeier, K. R.; Hwu, S.-J. *Inorg. Chem.* **1987**, *26*, 3297.  
(3) Komarneni, S.; Kozai, N.; Roy, R. J. *Mater. Chem.* **1998**, *8*, 1329.  
(4) Megaw, H. D. Z. *Kristallogr.* **1934**, *87*, 185.  
(5) Rothbauer, R.; Zigan, F.; O’Daniel, H. Z. *Kristallogr.* **1967**, *125*, 317.  
(6) Bosmans, H. J. *Acta Crystallogr.* **1970**, *B26*, 649.  
(7) Hanschild, V. Z. *Anorg. Allg. Chem.* **1963**, *324*, 15.

(8) Schoen, R.; Roberson, C. E. *Am. Mineral.* **1970**, *55*, 43.  
(9) Besserguenev, A. V.; Fogg, A. M.; Francis, R. J.; Price, S. J.; O’Hare, D.; Isupov, V. P.; Tolochko, B. P. *Chem. Mater.* **1997**, *9*, 241.  
(10) Fogg, A. M.; Freij, A. J.; Parkinson, G. M. *Chem. Mater.* **2002**, *14*, 232.  
(11) Lei, L.; Zhang, W.; Hu, M.; Zheng, H. J. *Solid State Chem.* **2006**, *179*, 3562.

**Table 1.** Results of Wet Chemical Analysis and TGA Data of the Bayerite-Based Li–Al–Cl LDH<sup>a</sup>

sample	Li <sup>+</sup> (wt.%)	Al <sup>3+</sup> (wt.%)	Cl <sup>-</sup> (wt.%)	% mass loss from TGA	approx. composition of sample
Li–Al–Cl LDH (bayerite-based)	2.5 (2.2)	26.9 (25.5)	9.6 (11.2)	41.8	[Li <sub>0.22</sub> Al <sub>0.66</sub> (OH) <sub>2</sub> ][Cl] <sub>0.22</sub> ·0.5H <sub>2</sub> O

<sup>a</sup> Values given in parentheses are calculated on the basis of the approximate composition given in the last column.

shape-selective intercalation of anions.<sup>12–14</sup> It is suggested that the origin of this shape selective intercalation lies in the unique structure of this material and in the cation ordering within the layers. A knowledge of the structure of the bayerite-based Li–Al LDHs should throw some light into these phenomena. In this paper, we take a close look at the products obtained by imbibition of Li salts into bayerite. We use Rietveld refinement and difference Fourier methods to look at the structure of the bayerite-based Li–Al–Cl LDH.

## Experimental Section

Bayerite was prepared by ammonia precipitation following a literature procedure.<sup>2</sup> Gibbsite was provided by Jawaharlal Nehru Aluminum Research Development and Design Center (JNARDDC; Nagpur, India). The Li–Al LDHs were prepared by soaking 0.5 g batches of bayerite or gibbsite in ~10 M LiX (X = Cl<sup>-</sup>, Br<sup>-</sup>, NO<sub>3</sub><sup>-</sup>, SO<sub>4</sub><sup>2-</sup>) solution (volume 40 mL) followed by hydrothermal treatment in a Teflon-lined autoclave (50% filling) at 125–140 °C (24 h).

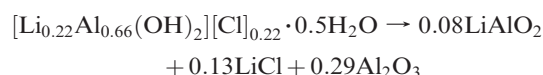
All samples were characterized by powder X-ray diffraction (PXRD; Bruker D8 Advance diffractometer, Cu K $\alpha$  radiation,  $\lambda$  = 1.5418 Å) operated in reflection geometry. Data were collected at a continuous scan rate of 1° min<sup>-1</sup> and a step size of 0.02° 2 $\theta$ . For Rietveld refinement, data were recorded over a 5–100° 2 $\theta$  range (step size of 0.02° 2 $\theta$ , counting time 10 s step<sup>-1</sup>). Unit cell parameters were refined using the PROSZKI program.<sup>15</sup> Simulation of powder diffraction patterns was carried out using POWDERCELL.<sup>16</sup>

The structure determination of bayerite-based Li–Al–Cl LDH was carried out by Rietveld refinement and difference Fourier methods using the GSAS<sup>17</sup> software package. For the refinement, a TCH–pseudo-Voigt line shape function (Profile Function 2) with eight variables was used to fit the experimental profile. The background was corrected using a 12-coefficient Chebyshev polynomial.

A complete chemical analysis was carried out for the Li–Al–Cl LDH to complement the structure solution of this phase (Table 1). The Li content in the LDH was estimated using flame photometry, Al content by gravimetric analysis, and Cl content by precipitation titration (Volhard's method).<sup>18</sup> The Li/Al ratio in the LDHs is less than the 0.5 expected of a stoichiometric compound. However, the Cl content is found to be equivalent to the Li content. The absence of any peaks due to the precursor Al(OH)<sub>3</sub> in the PXRD pattern of the sample obtained from bayerite indicates partial imbibition of Li to yield a composition of

[Li<sub>0.220.11</sub>Al<sub>0.66</sub>][Cl]<sub>0.22</sub> for the anhydrous LDH. The Li imbibition is substoichiometric, as the reaction was carried out at a higher temperature than that reported earlier for the intercalation of hydroxyl ions.<sup>22</sup>

The intercalated water content is obtained from the TGA data (Supporting Information SI.1), obtained using a Mettler Toledo TG/SDTA Model 851° system (30 – 800 °C, heating rate 5° min<sup>-1</sup>, flowing air). The LDH loses mass in two steps. The low-temperature mass loss is observed from 30 to ~260 °C and is attributed to a loss of adsorbed and intercalated water. The high-temperature mass loss (260 – 800 °C) is attributed to dehydroxylation and deamination. The total mass loss of 41.8% is consistent with the following reaction:



## Results and Discussion

The PXRD patterns of compounds obtained by the imbibition of Li salts into gibbsite and bayerite (Supporting Information SI.2–SI.5) can be indexed according to the cell parameters given in Table 2. The PXRD patterns of the two classes of LDHs differ significantly in the mid-2 $\theta$  region (30–60° 2 $\theta$ ). In this region are seen a series of peaks that can be indexed to the 11/ family of reflections of the hexagonal cell. The gibbsite-derived LDHs index to a two-layered hexagonal (2H) cell. The bayerite-derived LDHs, on the other hand, index to a three-layer hexagonal (3H) cell as well as a single-layered cell of monoclinic (1M) symmetry. This range of 2 $\theta$  values is affected the most by changes in the stacking sequence of the metal hydroxide layers and is therefore shown, in Figures 1 and 2, to exemplify the differences between the diffraction profiles of the gibbsite- and bayerite-based LDHs.

The layered nature of these materials implies that the metal hydroxide slabs may be stacked in a number of ways to give rise to different polytypes. This is well documented among the II–III LDHs.<sup>19,20</sup>

While the hexagonal symmetry of the gibbsite-based LDHs agrees with the structure refinements reported earlier,<sup>9</sup> the symmetry of the bayerite-based LDHs is ambiguous. The fact that (i) Li imbibition takes place topotactically, (ii) the precursor bayerite has a monoclinic symmetry, and (iii) the CO<sub>3</sub><sup>2-</sup> and SO<sub>4</sub><sup>2-</sup> intercalated bayerite-based Li–Al LDHs have in earlier papers been indexed to monoclinic symmetry<sup>21</sup> requires us to be cautious about accepting the hexagonal indexing and raises the question: are the LDHs derived from gibbsite and bayerite polytypes of the same symmetry; that is, do they differ only in their stacking sequences, or are they of two different symmetries altogether?

(12) Fogg, A. M.; Green, V. M.; Harvey, H. G.; O'Hare, D. *Adv. Mater.* **1999**, *11*, 1466.

(13) Fogg, A. M.; Dunn, J. S.; Shyu, S.-G.; Cary, D. R.; O'Hare, D. *Chem. Mater.* **1998**, *10*, 351.

(14) Lei, L.; Millange, F.; Walton, R. I.; O'Hare, D. *J. Mater. Chem.* **2000**, *10*, 1881.

(15) Lasocha, W.; Lewinski, K. *PROSZKI: A System of Programs for Powder Diffraction Data Analysis*, v. 2.4; Jagiellonian University: Krakow, Poland, 1994.

(16) Kraus, W.; Nolze, G. *POWDERCELL*, v. 2.4; Federal Institute for Materials Research and Training: Berlin, Germany, 2000.

(17) Larson, A. C.; Von Dreele, R. B. *General Structure Analysis System (GSAS)*, Los Alamos National Laboratory Report LAUR 86-748; Los Alamos National Laboratory: Los Alamos, NM, **2004**.

(18) *Vogel's Textbook of Quantitative Inorganic Analysis*, 4th ed.; Longman Group Ltd: Edinburgh Gate, U. K., 1978.

(19) Bookin, A. S.; Drits, V. A. *Clays Clay Miner.* **1993**, *41*, 551,558.

(20) Drits, V. A.; Bookin, A. S. *Layered Double Hydroxides: Present and Future*; Rives, V., Ed.; Novo Scientist: New York, 2001; pp 39–92.

(21) Sissoko, I.; Iyagba, R.; Sahai, R.; Biloen, P. *J. Solid State Chem.* **1985**, *60*, 283.

(22) Thiel, J. P.; Chiang, C. K.; Poeppelmeier, K. R. *Chem. Mater.* **1993**, *5*, 297.

Table 2. Unit Cell Parameters of the Li–Al LDHs

	bayerite-based LDH		
	gibbsite-based LDH two-layer hexagonal cell (2H)	three-layer hexagonal cell (3H)	monoclinic cell (1M)
Li–Al–Cl LDH	$a = 5.096 \text{ \AA}$ , $c = 15.17 \text{ \AA}$	$a = 5.096(1) \text{ \AA}$ , $c = 23.027(8) \text{ \AA}$	$a = 5.093(2) \text{ \AA}$ , $b = 8.838(7) \text{ \AA}$ , $c = 7.858(4) \text{ \AA}$ , $\beta = 102.37(6)^\circ$
Li–Al–Br LDH	$a = 5.090 \text{ \AA}$ , $c = 15.411 \text{ \AA}$	$a = 5.091(2) \text{ \AA}$ , $c = 26.90(2) \text{ \AA}$	$a = 5.086(2) \text{ \AA}$ , $b = 8.786(6) \text{ \AA}$ , $c = 7.919(2) \text{ \AA}$ , $\beta = 103.87(2)^\circ$
Li–Al–NO <sub>3</sub> LDH	$a = 5.080 \text{ \AA}$ , $c = 17.989 \text{ \AA}$	$a = 5.091(2) \text{ \AA}$ , $c = 26.90(2) \text{ \AA}$	$a = 5.087(3) \text{ \AA}$ , $b = 8.814(7) \text{ \AA}$ , $c = 9.12(1) \text{ \AA}$ , $\beta = 101.03(7)^\circ$
Li–Al–SO <sub>4</sub> LDH	$a = 5.096 \text{ \AA}$ , $c = 17.756 \text{ \AA}$	$a = 5.093(2) \text{ \AA}$ , $c = 26.02(3) \text{ \AA}$	$a = 5.100(9) \text{ \AA}$ , $b = 8.821(3) \text{ \AA}$ , $c = 8.83(1) \text{ \AA}$ , $\beta = 101.39(2)^\circ$

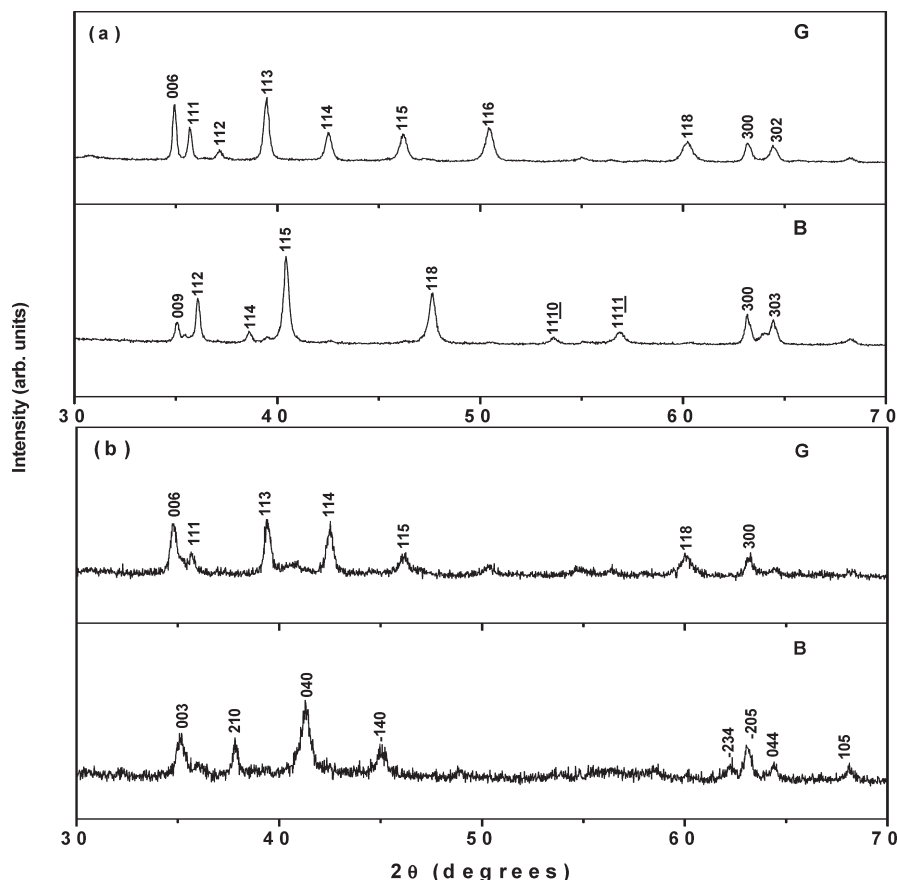


**Figure 1.** Powder X-ray diffraction patterns of the Li–Al–X LDHs derived from gibbsite and bayerite where X = (a) Cl<sup>−</sup> and (b) Br<sup>−</sup>. The low-angle region is omitted for clarity (G, gibbsite-based LDH; B, bayerite-based LDH).

To resolve this, we first examine the indexing of the bayerite-based LDHs. An earlier paper indexes the PXRD pattern of the Cl<sup>−</sup>-LDH to rhombohedral symmetry.<sup>10</sup> However, we observe that none of the patterns of the bayerite-based LDHs reported by these authors satisfy the reflection conditions characteristic of rhombohedral symmetry (that is,  $-h + k + l = 3n/h - k + l = 3n$ ). Therefore, the conclusion that these compounds belong to the rhombohedral symmetry is incorrect. However, the reflection conditions assumed by these authors<sup>10</sup> ( $00l = 3n$ ) are consistent with only 10 hexagonal space groups which can be grouped into five enantiomorphous sets:  $\{P3_1, P3_2\}$ ,  $\{P3_121, P3_221\}$ ,  $\{P6_2, P6_4\}$ , and  $\{P6_22, P6_422\}$ . We carried out a Le Bail fit of the Li–Al–Cl LDH in one of these space groups ( $P6_2$ ). Although the resulting fit is good ( $R_{wp} = 0.167$ ), a comparison with a similar fit done using monoclinic symmetry ( $C2/m$ ;  $R_{wp} = 0.136$ ) shows that the observed split in the high-angle peak ( $64\text{--}65^\circ 2\theta$ ) can be accounted for only by the monoclinic symmetry. The peak in this region exhibits a shoulder at  $64.6^\circ 2\theta$ , which can be indexed to the 204

reflection of the monoclinic system. The PXRD pattern in this region with the Bragg positions corresponding to the monoclinic and hexagonal symmetries (Figure 3) clearly shows that the split in the peak is better accounted for by the monoclinic indexing. We therefore conclude that the Li–Al–Cl LDH crystallizes with monoclinic symmetry.

In the case of the bayerite-based Li–Al–Br LDH, the pattern indexes better to a monoclinic cell rather than a hexagonal cell (Table 3). In this case, it appears that the distortion from hexagonal symmetry is greater than in the other Li–Al LDHs.

There is a need for a complete structural characterization of the bayerite-based LDHs, as such a study has not been performed until now. We take the Li–Al–Cl LDH as an illustrative example, it being the simplest case of that of a monatomic anion in the interlayer region. Furthermore, the PXRD pattern of this material exhibits uniformly broadened peaks, a feature indicative of an ordered crystal. We therefore carry out a structure solution of this phase.

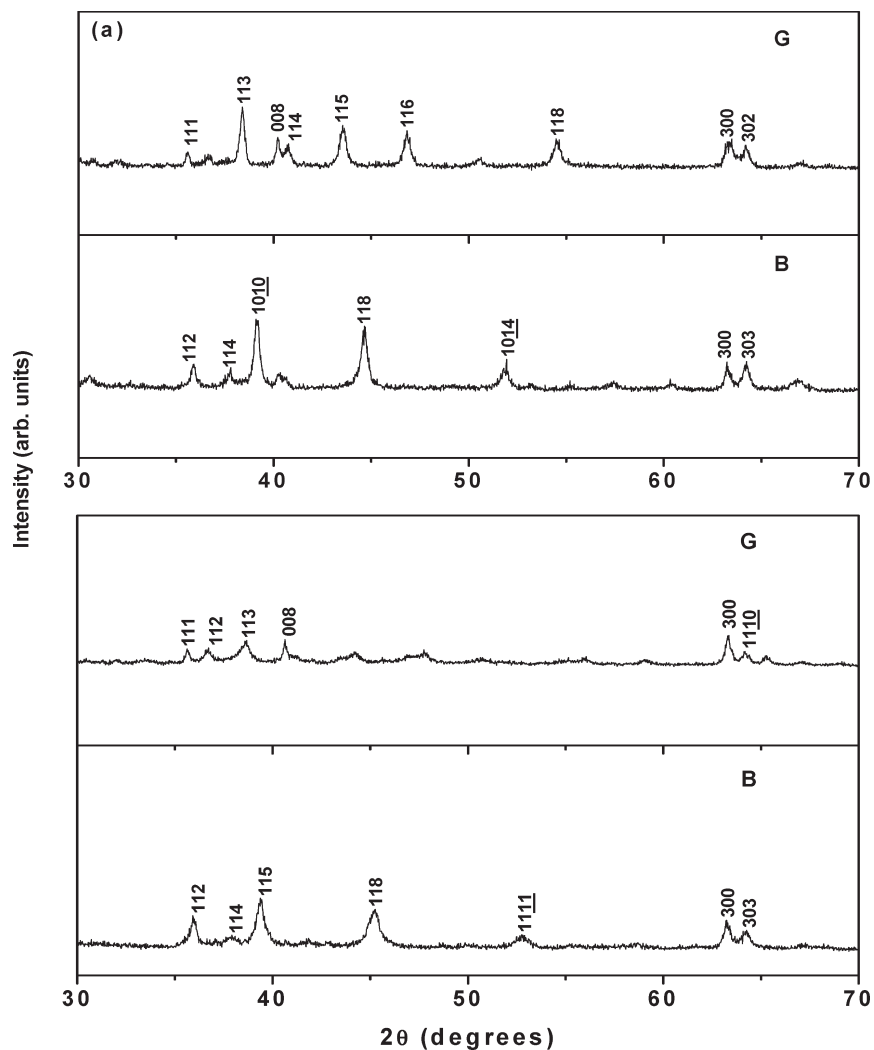


**Figure 2.** Powder X-ray diffraction patterns of the Li–Al–X LDHs derived from gibbsite and bayerite where X = (a)  $\text{NO}_3^-$  and (b)  $\text{SO}_4^{2-}$ . The low-angle region is omitted for clarity (G, gibbsite-based LDH; B, bayerite-based LDH).

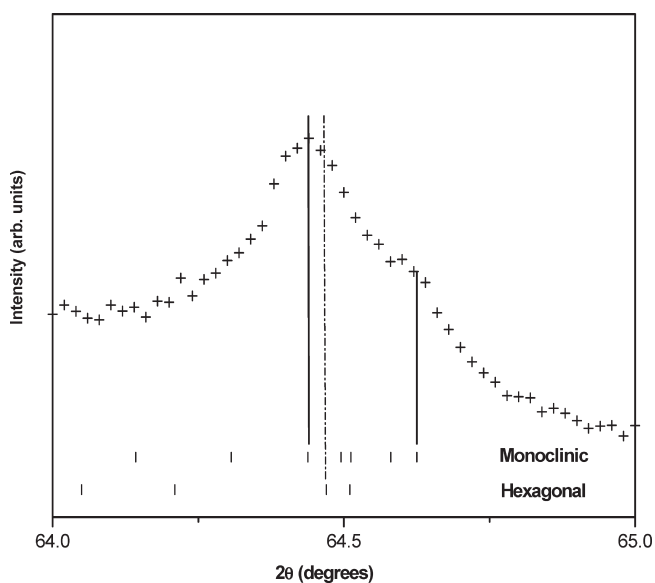


**Figure 3.** PXRD pattern of the bayerite-based Li–Al–Cl LDH expanded in the region 64–65°  $2\theta$ .

**Table 3.** Observed and Calculated  $2\theta$  Values of the Bayerite-Based Li–Al–Br LDH

$2\theta$ (obsd; deg)	monoclinic cell <sup>a</sup>		hexagonal cell <sup>b</sup>	
	$2\theta$ (calcd; deg)	$hkl$	$2\theta$ (calcd; deg)	$hkl$
11.51	11.50	001	11.52	003
23.17	23.12	002	23.17	006
35.12	34.98	003	35.06	009
37.85	37.81	210	37.31 <sup>c</sup>	108
41.32	41.05 <sup>c</sup>	040	41.15 <sup>c</sup>	201
45.10	45.14	–140	45.04	117
62.29	62.24	–234	62.49 <sup>c</sup>	217
63.09	63.04	–205	63.31 <sup>c</sup>	300
64.41	64.35	044	64.37	2012
68.05	68.01	105	67.88	2013

<sup>a</sup>  $a = 5.086(2)$  Å,  $b = 8.786(6)$  Å,  $c = 7.919(2)$  Å,  $\beta = 103.87(2)^\circ$ . <sup>b</sup>  $a = 5.084(4)$  Å,  $c = 23.01(4)$  Å. <sup>c</sup> Reflections exhibiting poor agreement with the observed positions.

The monoclinic structure (space group  $C2/m$ ) of  $\text{LiAl}_2(\text{OH})_7 \cdot 2\text{H}_2\text{O}$  given in the paper of Thiel and co-workers<sup>22</sup> was used as the structure model for Rietveld refinement. The  $C2/m$  space group allows for the placement of interlayer

atoms in any of the five special positions:  $2c$  (0, 0, 0.5),  $2d$  (0, 0.5, 0.5),  $4f$  (0.25, 0.25, 0.5),  $4h$  (0,  $y$ , 0.5), and  $4i$  ( $x$ , 0,  $z$ ) or the general position  $8j$  ( $x$ ,  $y$ ,  $z$ ). A POWDERCELL simulation of the observed pattern with this structure model gave a reasonable fit to the observed pattern after placing the interlayer atoms in the  $2c$  and  $4h$  positions as given in Supporting Information SI.6. This structure model was therefore used for Rietveld refinement. Precise lattice parameters used for the refinement were obtained by first carrying out a Le Bail refinement. Initially, the SOFs of the Li, Al, and layer O atoms were fixed at 1. The scattering factors of all of the  $\text{OH}^-$  and  $\text{H}_2\text{O}$  were considered to be that of  $\text{O}^{2-}$  ions. Initial refinement of scale, background, profile parameters, and occupancy factors of interlayer atoms resulted in reasonably low  $R_{\text{wp}}$  and  $R_{\text{p}}$  values of 0.21 and 0.16, respectively (Supporting Information SI.7), indicating that the starting model is essentially correct. A difference Fourier map was computed at this stage and showed an electron density of  $\sim 1.2 \text{ e } \text{\AA}^{-3}$  at an  $8j$  position (0.327, 0.170, 0.5). The interlayer atoms were fixed in these positions and their occupancy factors refined. Two further cycles of refinement were carried out, and the resulting difference Fourier map indicated significant electron density in the interlayer region at the  $4h$  and  $4i$  sites. The interlayer atoms were distributed over the  $8j$

and  $4h$  and  $4i$  positions and the occupancy factors allowed to freely refine. The SOF of the atom in the  $8j$  position roughly matched that calculated for interlayer  $\text{H}_2\text{O}$  (TG data: Supporting Information SI.1; Table 1), while the sum of the occupancy factors of the atoms in the  $4h$  and  $4i$  positions corresponded to that expected of interlayer  $\text{Cl}^-$ . The  $\text{H}_2\text{O}$  oxygen was therefore assigned to the  $8j$  position, and the  $\text{Cl}^-$  ions were distributed over the  $4h$  and  $4i$  sites. A further cycle of refinement showed no significant residual electron density in the interlayer region ( $\sim 0.3 \text{ e } \text{\AA}^{-3}$ ). The maximum electron density in the difference Fourier map corresponding to the difference profile of the final cycle of refinement (Figure 4) was  $\sim 0.8 \text{ e } \text{\AA}^{-3}$ . The final refined atomic coordinates are given in Table 4, and the refinement conditions are given in Table 5. The thermal parameter of the Cl atom in the  $4h$  site is higher than that of the Cl atom in  $4i$  site. This could be due to either of the following: (i) the  $4h$  site is actually occupied by a lighter atom, or (2) the  $4h$  site has a lower occupancy. The distribution of atoms as in Table 4 yielded the lowest  $R$  values. Readjusting the site occupancies yielded comparable values of the thermal parameters for the atoms in the two sites, but higher  $R$  values. The structure given in Table 4 yielded the lowest  $R$  value. Further, the refinement yields a formula of  $[\text{Li}_{0.23}\text{Al}_{0.66}(\text{OH})_2][\text{Cl}]_{0.23} \cdot 0.60\text{H}_2\text{O}$ , which

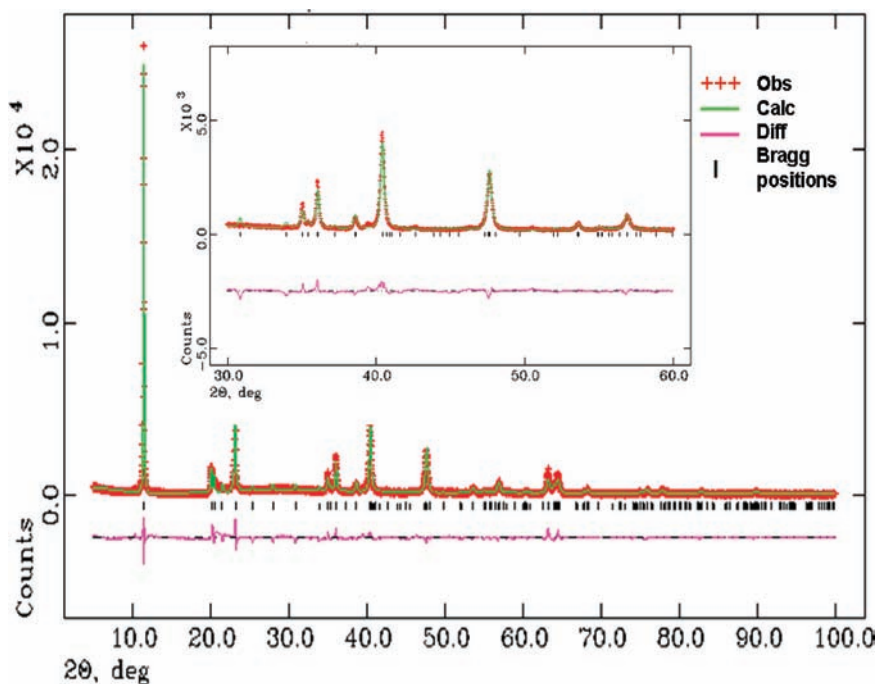


**Figure 4.** Final Rietveld fit of the observed PXRD profile of the bayerite-based Li–Al–Cl LDH. In the inset is given the zoomed-in image of the fit in the  $2\theta$  range  $30\text{--}60^\circ$ .

**Table 4.** Refined Unit Cell and Atomic Parameters after the Final Cycle of Refinement

atom type	Wyckoff position <sup>a</sup>	$x$	$y$	$z$	SOF	$U_{\text{iso}}/\text{\AA}^2$
Li	$2a$	0	0	0	0.70	0.025
Al	$4g$	0	0.3313(9)	0	1.0	0.00573
O1	$8j$	0.8661(15)	0.1698(6)	0.1278(5)	1.0	0.00108
O2	$4i$	0.3594(20)	0.0	0.1263(10)	1.0	0.04106
O3	$8j$	0.2529(28)	0.1580(17)	0.5018(16)	0.452	0.02277
Cl1	$4h$	0.0	0.183(5)	0.5	0.167	0.08421
Cl2	$4i$	0.6442(35)	0.0	0.4985(29)	0.186	0.01662

<sup>a</sup>  $a = 5.0992(5) \text{ \AA}$ ,  $b = 8.8215(8) \text{ \AA}$ ,  $c = 7.8669(5) \text{ \AA}$ ,  $\beta = 102.51(1)^\circ$ .

approximates to that obtained by chemical analysis. It may however be noted that small variations in electron density cannot be interpreted with certainty, and therefore

**Table 5.** Crystal Data and Structure Refinement Parameters of the Bayerite-Based Li–Al–Cl LDH

empirical formula	[LiAl <sub>2</sub> (OH) <sub>6</sub> ]Cl·H <sub>2</sub> O
cryst syst	monoclinic
space group	C2/m
cell parameters/Å	<i>a</i> = 5.0992(5), <i>b</i> = 8.8215(8), <i>c</i> = 7.8669(5), $\beta$ = 102.51(1)
vol/Å <sup>3</sup>	345.47(2)
data points	4750
reflms fitted	203
params refined	49
<i>R</i> <sub>wp</sub>	0.1723
<i>R</i> <sub>p</sub>	0.1264
<i>R</i> ( <i>F</i> <sup>2</sup> )	0.1095
<i>R</i> <sub>exp</sub>	0.049

the assignment of sites to the O and Cl atoms here are indicative rather than being definitive.

The relevant bond distances and bond angles are given in Table 6. It can be seen that the LiO<sub>6</sub> and AlO<sub>6</sub> octahedra are distorted, but the Al–O distances are comparable with that in bayerite.

The structures of the gibbsite-based and bayerite-based LDHs are compared in Figure 5. The gibbsite-based LDH crystallizes in hexagonal symmetry with the layers stacked in an ABBA AB... manner giving rise to prismatic sites in the interlayer region.<sup>9</sup> The stacking sequence in the bayerite-based Li–Al–Cl LDH may be understood by comparing it with that of the precursor bayerite. A look at the cell parameters of the LDH (*a* = 5.099 Å, *b* = 8.821 Å, *c* = 7.867 Å,  $\beta$  = 102.51°) and that of bayerite (*a* = 5.062 Å, *b* = 8.671 Å, *c* = 4.713 Å,  $\beta$  = 90.27°) shows that the main difference between the two, apart from the increase in the *c* parameter, is in the monoclinic angle  $\beta$ . More important than

**Table 6.** Selected Bond Distances and Bond Angles in Bayerite-Based Li–Al–Cl LDH

	gibbsite	gibbsite based LDH <sup>a</sup>	bayerite		bayerite-based LDH		bayerite-based LDH
Al–O1	1.862	1.911	1.738	Al–O1	1.951(7)	Cl1–O2	4.009(31)
Al–O2	1.930	1.911	1.899	Al–O1	1.951(7)	Cl1–O1	4.015(15)
Al–O3	1.881	1.911	1.901	Al–O1	1.919(7)	Cl1–O1	4.015(15)
Al–O4	1.947	1.898	1.922	Al–O1	1.919(7)	Cl2–O2	2.980(22)
Al–O5	1.922	1.898	1.984	Al–O2	2.006(7)	Cl2–O2	3.003(24)
Al–O6	1.890	1.898	2.063	Al–O2	2.006(7)	Cl2–O1	3.621(19)
Li–O1		2.057		Li–O1	2.004(6)	Cl2–O1	3.684(20)
Li–O2		2.057		Li–O1	2.004(6)	Cl2–O1	3.621(19)
Li–O3		2.057		Li–O1	2.004(6)	Cl2–O1	3.684(20)
Li–O4		2.057		Li–O1	2.004(6)	O3–O2	3.450(15)
Li–O5		2.057		Li–O2	1.886(9)	O3–O2	3.414(14)
Li–O6		2.057		Li–O2	1.886(9)	O3–O1	3.469(13)
				Cl1–O1	2.861(4)	O3–O1	3.481(15)
				Cl1–O1	2.861(4)	O3–O1	3.104(12)
				Cl1–O2	4.009(31)	O3–O1	3.169(14)

Bond Angles/deg for the Bayerite-Based LDH

O1–Al1–O1	97.80(28)	O1–Al1–O1	86.1(5)	O1–Li1–O1	83.31(35)
O1–Al1–O2	99.0(4)	O1–Al1–O2	94.82(28)	O1–Li1–O1	96.69(35)
O2–Al1–O2	84.2(6)	O1–Li1–O2	97.67(19)		

<sup>a</sup> Values obtained from ref 9.

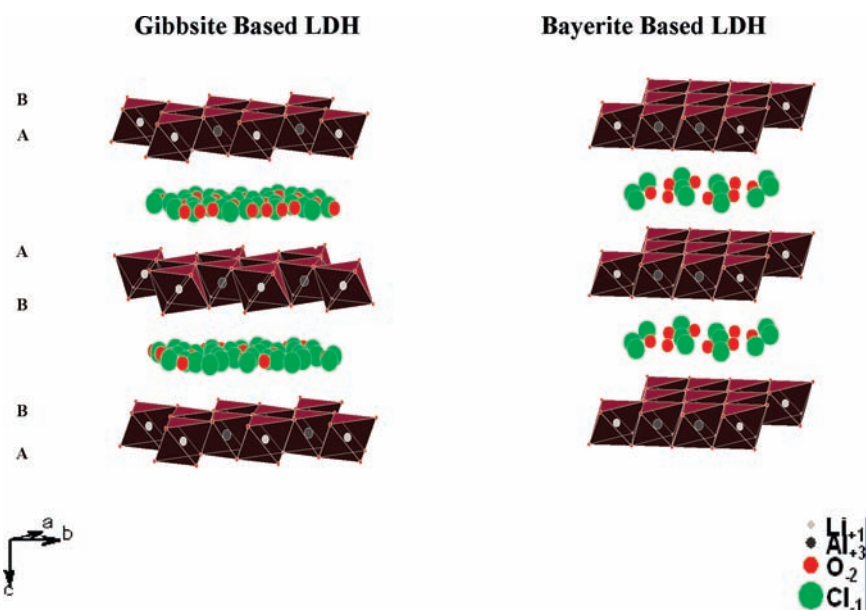


**Figure 5.** Schematic of the structures of the gibbsite-based and bayerite-based Li–Al–Cl LDHs.

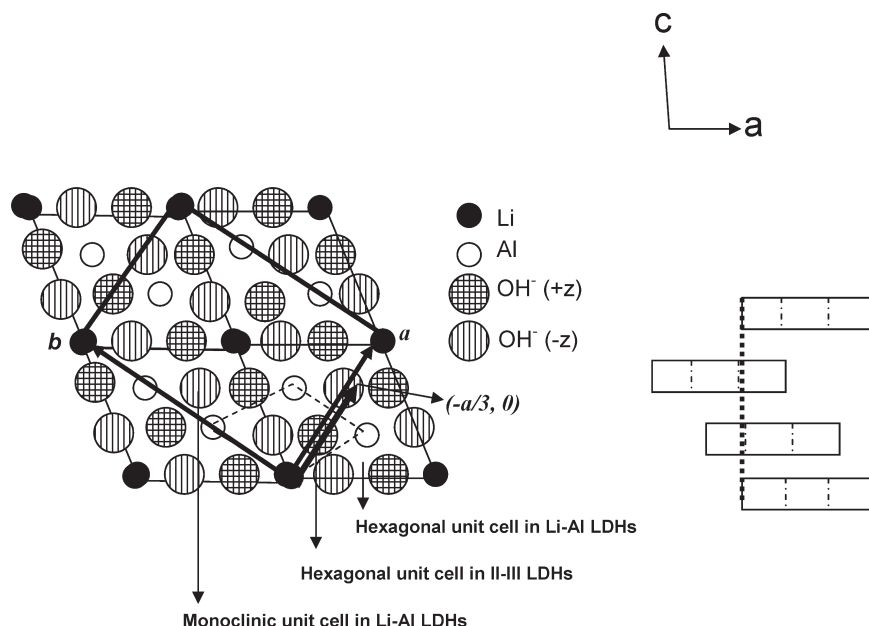


**Figure 6.** Schematic showing the projection in the  $a$ - $b$  plane of the Li-Al LDH with the inter-relationships between the unit cells of different symmetry. The dotted line represents the hexagonal unit cell in II-III LDHs. One quadrant of the figure in the left panel represents the hexagonal unit cell in the Li-Al LDHs. The bayerite-based Li-Al-Cl LDH, however, is better described by the monoclinic unit cell described by the bold lines. The vector  $(-a/3, 0)$  defines the relative translation within the  $a$ - $b$  plane of successive layers. On the right is a schematic of the elevation.

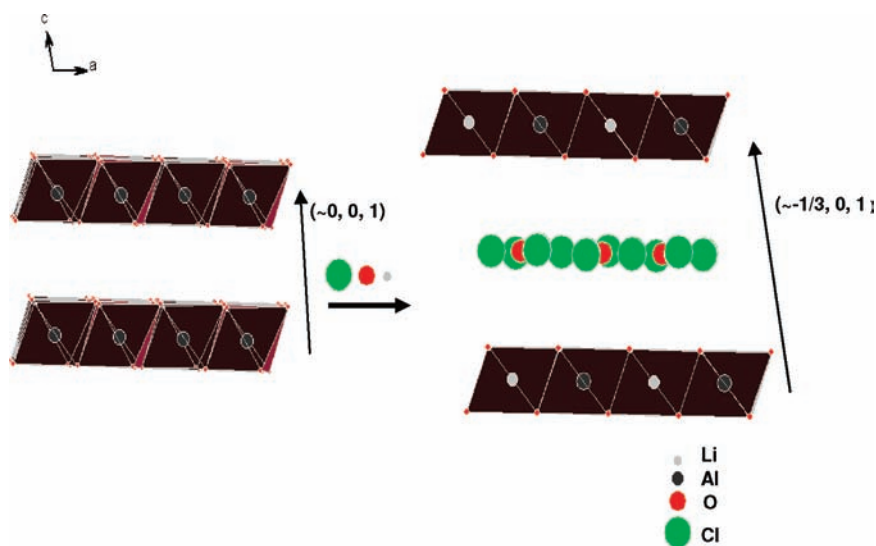


**Figure 7.** Schematic showing the imbibition process of LiCl into bayerite to give the bayerite-based Li-Al-Cl LDH.

the exact crystal structure is an understanding of how the successive metal hydroxide layers are stacked with respect to each other. Such an analysis enables the comparison of structures of different symmetries and their interrelation. The cell parameters of the bayerite-based Li-Al-Cl LDH yield a translation of  $(-0.3302, 0, 1)$  between successive metal hydroxide layers (Figure 6).<sup>23</sup> Figure 6a is a schematic of the projection in the  $a$ - $b$  plane of the LDH structure, showing the interrelationships between the different unit cells. The conventional unit cell chosen when no cation ordering is assumed is also shown for comparison. Cation ordering requires the choice of a larger hexagonal unit cell. The slight deviation from hexagonal symmetry leads to the choice of the

one-layer monoclinic unit cell. A translation of  $(\sim -1/3, 0, 1)_m$  ( $m$ : monoclinic) corresponds to a translation of  $(\sim 2/3, \sim 2/3, 1/3)_h$  ( $h$ : hexagonal) of the hexagonal cell. An exact translation of  $(-1/3, 0, 1)_m / (2/3, 2/3, 1/3)_h$  would lead to a three-layer hexagonal cell and explains the three-layer pseudohexagonal indexing. The topotactic mechanism of imbibition is reflected in the similarity of the  $a$  and  $b$  parameters of the LDH with that of the precursor. However, intercalation of  $\text{Cl}^-$  ions and water molecules in the interlayer region causes the layers to translate along the  $a$  direction, the stacking vector going from  $(-0.0043, 0, 1)$  in bayerite to  $(-0.3302, 0, 1)$  in the LDH (Figure 7).

The commonly encountered polytype ( $3R_1$ ) among the II-III LDHs corresponds to a structure where the successive metal hydroxide layers are translated by the stacking vector  $(2/3, 1/3, 1/3)$ . Other polytypes can be envisaged with

(23) Britto, S.; Thomas, G. S.; Kamath, P. V.; Kannan, S. *J. Phys. Chem. C* **2008**, *112*, 9510.

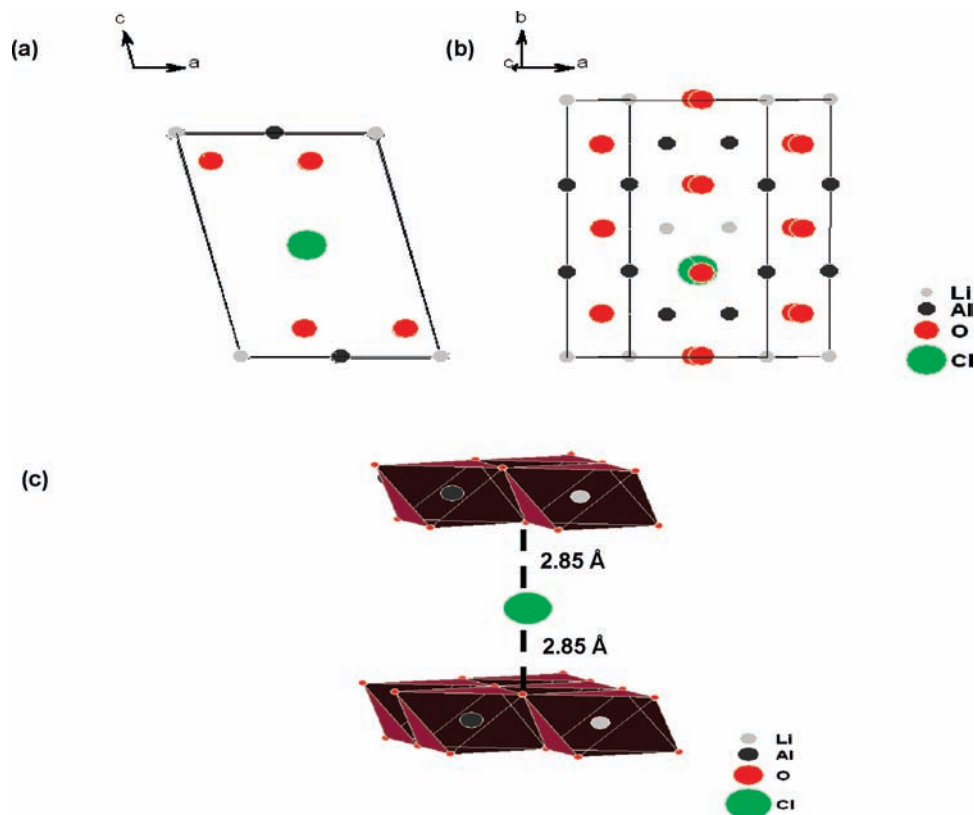


**Figure 8.** (a) Unit cell of the bayerite-derived Li–Al–Cl LDH (side view), (b) view perpendicular to the  $a$ – $b$  plane, (c) polyhedral representation of a part of the structure of the Li–Al–Cl LDH showing the 2-fold coordination of the  $\text{Cl}^-$  ion in the interlayer region.

stacking vectors of the type  $(\pm 2/3, \pm 1/3, 1/3)$ .<sup>19,20</sup> These translations generate either trigonal prismatic or octahedral interlayer sites. It is further pointed out that the LDHs select for anions having a molecular symmetry which matches with the local symmetry of the interlayer sites.<sup>24,25</sup> The shape selectivity exhibited by the gibbsite-based LDHs<sup>12–14</sup> is likely a result of the unique interlayer environment engendered by cation ordering and positional disorder of the interlayer atoms. The chemical pertinence of different polytypes arises from their differing interlayer site symmetries, which determines the affinities of the polytypes for different anions.

We therefore ask the question: what is the local symmetry of the interlayer site, when the layers are stacked with the stacking vector  $(\sim -1/3, 0, 1)_m$ ? Figure 8a,b show the side and top views (perpendicular to the  $a$ – $b$  plane) of the unit cell of the bayerite-derived LDH. Figure 8b shows that the translation of  $(\sim -1/3, 0, 1)$  results in destroying cation ordering perpendicular to the  $a$ – $b$  plane. The symmetry of the interlayer anion in such an environment may be deduced by examining the bond lengths and bond angles around the intercalated atoms (Table 6).

The intercalated Cl atoms are in two different symmetry-distinct sites ( $4h$  and  $4i$ ). The Cl atoms in both positions exhibit only two short contacts with the layer hydroxyls which fall within the range of H-bonding distances (2.8–3.0 Å). The other distances are in excess of 4 Å. The  $\text{Cl}^-$  atoms in the interlayer are in 2-fold coordination (Figure 8c). The water oxygens exhibit six short contacts (3.2–3.4 Å) and lie within approximately prismatic

interstitial sites. The nonideal nature of these sites results in the chloride ions preferring to occupy sites of linear symmetry in order to maximize hydrogen bonding with the hydroxyl groups of the layer. In contrast, in the gibbsite-based LDH, the extensive positional disorder of the atoms in the interlayer (Figure 5) precludes a precise definition of the coordination for the  $\text{Cl}^-$  ion.

Insights into the structure of the bayerite-based Li–Al LDHs has important implications for the intercalation chemistry and anion exchange reactions of these compounds. Earlier studies into the kinetics of imbibition of Li salts into bayerite and gibbsite polymorphs showed that, although there are some differences, no clear mechanistic trends are apparent. Our investigations<sup>23</sup> reveal that by far the most significant difference between the bayerite- and gibbsite-based LDHs is with respect to affinity for the carbonate ion. While there are numerous reports on the existence of bayerite-based carbonate Li–Al LDHs,<sup>1</sup> there are no reports on the gibbsite-based carbonate LDHs. It appears that the bayerite-based Li–Al LDHs have a higher affinity for carbonate than the gibbsite-based Li–Al LDHs. It is well-known that the II–III LDHs have a high affinity for the carbonate ion. This is largely due to the stabilizing H-bonding interactions that arise due to matching of the symmetry of the carbonate ion with the prismatic interlayer sites of these compounds. Efforts are ongoing in our lab to see if such a phenomenon contributes to the differences in affinity toward carbonate among the Li–Al LDHs.

Further insights into the influence of the intercalated anion on the symmetry of the LDH may be had by looking at the structures of the bayerite-based LDHs intercalated with other anions ( $\text{NO}_3^-$ ,  $\text{SO}_4^{2-}$ , and  $\text{Br}^-$ ). Attempts to make

(24) Radha, A. V.; Shivakumara, C.; Kamath, P. V. *J. Phys. Chem. B* 2007, 111, 3411.

(25) Radha, S.; Kamath, P. V. *Cryst. Growth Design* 2009, 9, 3197.



better ordered materials to enable structure analysis are currently in progress.

In conclusion, this work shows that the gibbsite- and bayerite-based Li–Al LDHs are not two different polytypes of the same symmetry but actually crystallize in structures of different crystal symmetries.

**Acknowledgment.** The authors thank the Department of Science and Technology (DST), Government of India,

for financial support. P.V.K. is a recipient of the Ramanana Fellowship of the DST. S.B. thanks the University Grants Commission for the award of a Senior Research Fellowship (NET). The authors thank the JNARDDC, Nagpur, for a generous gift of gibbsite.

**Supporting Information Available:** Additional figures and tables. This material is available free of charge via the Internet at <http://pubs.acs.org>.